

## 两个 salen 型卤代希夫碱 Ni(II)配合物的合成、 晶体结构及 Hirshfeld 表面分析

吴 琼<sup>\*,1,2</sup> 唐亚芳<sup>1</sup> 资巧丽<sup>1</sup>

(<sup>1</sup>昆明学院化学化工学院,昆明 650214)

(<sup>2</sup>云南省塑料薄膜制品工程技术研究中心,昆明 650214)

**摘要:** 通过硝酸镍与卤代希夫碱在甲醇溶液中反应,合成了 2 个 Ni(II)希夫碱配合物[Ni(3,5-Cl-salcy)] (**1**) 和[Ni(3-Cl-salcy)] (**2**), (3,5-Cl-salcyH<sub>2</sub>=*N,N'*-(±)-双(3,5-二氯水杨基)-1,2-环己二胺; 3-Cl-salcyH<sub>2</sub>=*N,N'*-(±)-双(3-氯水杨基)-1,2-环己二胺)。通过 X 射线衍射测定了 2 个配合物的结构。结构分析表明 2 个配合物的基本单元均为 Ni(II)离子通过与希夫碱配体的[N<sub>2</sub>O<sub>2</sub>]原子配位构成相似的平面型单核配合物。Platon 软件分析表明配合物 **1** 中并不存在任何氢键, 配合物 **2** 也仅存在非经典氢键。通过 Hirshfeld 表面分析法对 2 个配合物晶体结构中弱交换作用的分析结果表明,虽然卤原子构成的氢键相对较弱,但是 C-H...X 在稳定三维超分子晶体结构中起着非常重要的作用;此外,通过 2 个配合物的对比发现,配体中卤原子数量的不同对于晶体中弱交换作用的占比可以起到非常重要的影响。

**关键词:** 卤代希夫碱; 晶体结构; 弱交换作用; Hirshfeld 表面分析

中图分类号: O614.81·3

文献标识码: A

文章编号: 1001-4861(2019)08-1477-08

DOI: 10.11862/CJIC.2019.189

## Syntheses, Crystal Structures, Hirshfeld Surface Analysis of Two Salen-Type Halogenated Schiff-Base Ni(II) Complexes

WU Qiong<sup>\*,1,2</sup> TANG Ya-Fang<sup>1</sup> ZI Qiao-Li<sup>1</sup>

(<sup>1</sup>College of Chemistry and Chemical Engineering, Kunming University, Kunming 650214, China)

(<sup>2</sup>Yunnan Engineering Technology Research Center for Plastic Films, Kunming 650214, China)

**Abstract:** The reaction between nickel nitrate and halogenated salen-type Schiff-base ligand in methanol solution led to the isolation of two new salen nickel(II) complexes [Ni(3,5-Cl-salcy)] (**1**) and [Ni(3-Cl-salcy)] (**2**), where 3,5-Cl-salcyH<sub>2</sub>=*N,N'*-(±)-bis(3,5-dichlorosalicylidene)cyclohexane-1,2-diamine and 3-Cl-salcyH<sub>2</sub>=*N,N'*-(±)-bis(3-chlorosalicylidene)cyclohexane-1,2-diamine. The crystal structures of complexes **1** and **2** were structurally characterized by single-crystal X-ray diffraction. Structural analysis reveals that the basic units of both complexes all consist of one nickel(II) ion in [N<sub>2</sub>O<sub>2</sub>] coordination sphere, forming similar square planar geometries. PLATON software analysis indicates that there is not any hydrogen bond exists in the crystal structure of **1**, and only unclassical hydrogen bonds exist in **2**. However, Hirshfeld surface analysis shows that, although the strength of halogen atoms formed hydrogen bonds are weak, the C-H...X bonds play an important role in stabilization of three-dimensional networks of both complexes. Moreover, by comparison of the two complexes, we found that the difference in the number of halogen atoms in the ligand can have a very important influence on the proportion of weak exchange in the crystal. CCDC: 1892682, **1**; 1855958, **2**.

**Keywords:** halogenated Schiff-base; crystal structure; weak molecular interactions; Hirshfeld surface analysis

收稿日期: 2019-02-15。收修改稿日期: 2019-06-14。

国家自然科学基金(No.31760257),云南省科技厅高校联合项目(No.2017FH001-002),昆明学院化学化工类大学生创新实践科学研究项目(No.HXHG1808),高原地区农用塑料薄膜材料与制品研究开发(平台)(No.2016DH006)资助。

\*通信联系人。E-mail: wuqiongkm@163.com

## 0 Introduction

Supramolecular chemistry is an important research field including multiple-subject ranging from pharmaceuticals to nanotechnology industries<sup>[1-4]</sup>. During the last decade, great efforts have been devoted to the rational design and synthesis of supramolecular aggregates with desired structure and properties<sup>[5-7]</sup>.

Different supramolecular interaction resulting in different solid geometry and even physicochemical properties, such as activity of pharmaceutical ingredients (APIs), magnetic behavior of molecular magnets. As is known to all, chemical reactivity and properties of organic compound are differed wildly by substitution of halogen atom<sup>[8-10]</sup>. Furthermore, halogen atom has recently been recognized as an important factor in mediation the supramolecular network of crystalline materials<sup>[11-12]</sup>. However, compared with the classic hydrogen-bond interactions, the contact formed by halogen atom is much weaker, so it is difficult to carry out qualitative and quantitative research, especially for the N- and O- rich ligands constructing supramolecular complex<sup>[13-15]</sup>. Hence, related work is still at a very early stage.

Therefore, establishing a series of halogenated ligands constructing complexes with similar structure and composition is a fundamental way for detailed recognition of the intermolecular interactions formed by halogen atom. In this aspect, tetradentate Schiff base (salen) complex is an ideal candidate, not only because the complex has diverse structures and tunable constitution<sup>[16-18]</sup>, but also because it is a well researched subject. Thus, subtle difference between analogs can be easily detected and studied<sup>[19-20]</sup>.

Based on the aforementioned considerations, recently, we have initiated exploitation of the

relationship between the composition of salen-type halogenated Schiff-base ligands and the structure of their complexes. Herein, we specifically introduced isomorphous halogenated salen as starting material, and isolated two nickel(II) complexes [Ni(3,5-Cl-salcy)] (**1**) and [Ni(3-Cl-salcy)] (**2**) (3,5-Cl-salcyH<sub>2</sub>=*N,N'*-(±)-bis(3,5-dichlorosalicylidene)cyclohexane-1,2-diamine and 3-Cl-salcyH<sub>2</sub>=*N,N'*-(±)-bis(3-chlorosalicylidene)cyclohexane-1,2-diamine). Theoretical analysis results reveal that halogen atoms play a key role in stabilizing the solid structures of title complexes.

## 1 Experimental

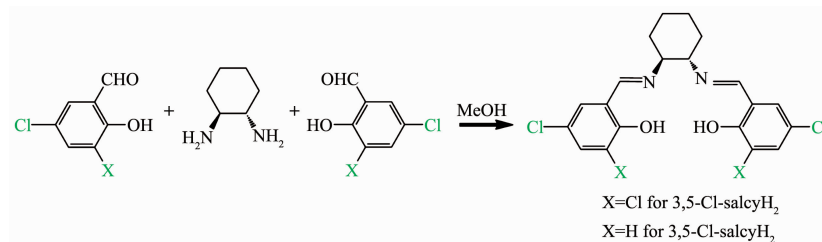
### 1.1 Material and methods

All chemicals were commercially available and used without further purification. Elemental analyses (C, H and N) were carried out on a Perkin-Elmer 240C instrument. Ni was analyzed on a PLASMA-SPEC(I) ICP atomic emission spectrometer. IR spectra were recorded in a range of 400~4 000 cm<sup>-1</sup> on an Alpha Centaur FT/IR Spectrophotometer using KBr pellets. <sup>1</sup>H NMR spectra have been recorded by using Bruker 600 MHz Digital NMR Spectrometer resonance instrument (AVANCE III 600 MHz).

### 1.2 Synthesis

#### 1.2.1 Synthesis of halogenated Schiff base ligand

The halogenated tetradentate Schiff base ligand 3,5-Cl-salcyH<sub>2</sub> and 3-Cl-salcyH<sub>2</sub> were prepared by mixing salicylaldehyde (3,5-dichlorosalicylaldehyde and 3-chlorosalicylaldehyde for 3,5-Cl-salcyH<sub>2</sub> and 3-Cl-salcyH<sub>2</sub>, respectively) (0.2 mmol) and 1,2-diaminocyclohexane (0.012 mL, 0.1 mmol, mixture of *cis*- and *trans*- form) in 30 mL of methanol. The obtained solution was stirred and refluxed at 80 °C for three hours, then the solvent was removed by rotary evaporator to give yellow powder product (Scheme 1).



Scheme 1 Schematic drawing of halogenated tetradentate Schiff base ligands 3,5-Cl-salcyH<sub>2</sub> and 3-Cl-salcyH<sub>2</sub>

3,5-Cl-salcyH<sub>2</sub>: Yield: 0.035 2 g (75%). Elemental analysis for C<sub>20</sub>H<sub>18</sub>Cl<sub>4</sub>N<sub>2</sub>O<sub>2</sub>(%): C: 52.2; H: 3.94; N: 6.08. Found(%): C: 51.2; H: 3.93; N: 6.13. <sup>1</sup>H NMR (600 MHz, methanol-d<sub>4</sub>): δ 8.38 (d, *J*=62.4 Hz, 1H, -N=CH-), 7.48~7.10 (m, 2H, ArH), 4.50 (s, 1H, Ar-OH), 3.85 (dt, *J*=6.7, 3.1 Hz, 1H, -C\*H-), 2.06~1.77 (m, 2H, -CH<sub>2</sub>-), 1.76~1.18 (m, 2H, -CH<sub>2</sub>-). FT-IR (cm<sup>-1</sup>): 3 419 (O-H), 1 598 (C=N), 1 389 (-CH<sub>2</sub>-).

3-Cl-salcyH<sub>2</sub>: Yield: 0.034 3 g (86%). Elemental analysis for C<sub>20</sub>H<sub>20</sub>Cl<sub>2</sub>N<sub>2</sub>O<sub>2</sub>(%): C: 61.39; H: 5.15; N: 7.15. Found(%): C: 61.57; H: 4.60; N: 7.27. <sup>1</sup>H NMR (600 MHz, methanol-d<sub>4</sub>): δ 8.38 (d, *J*=68.5 Hz, 1H, -N=CH-), 7.57~6.92 (m, 2H, ArH), 6.65 (dt, *J*=34.9, 7.8 Hz, 1H, Ar-OH), 4.09~3.68 (m, 1H, -C\*H-), 2.19~1.79 (m, 2H, -CH<sub>2</sub>-), 1.78~1.43 (m, 2H, -CH<sub>2</sub>-). FT-IR (cm<sup>-1</sup>): 3 432 (O-H), 1 598 (C=N), 1 389 (-CH<sub>2</sub>-).

### 1.2.2 Synthesis of [Ni(3,5-Cl-salcy)] (1)

Ni(NO<sub>3</sub>)<sub>2</sub>·6H<sub>2</sub>O (0.060 0 g, 0.2 mmol) was dissolved in 10 mL methanol, and the solution was added to 20 mL of a methanolic solution of 3,5-Cl-salcyH<sub>2</sub> (0.031 6 g, 0.1 mmol), the resulting dark red suspension was stirred for 2 h. After cooling, the reddish filtrate was sealed in a beaker and kept undisturbed at room temperature. The red block crystals of complex **1** were afforded after one week. Yield: 35%. Anal. Calcd. for C<sub>20</sub>H<sub>16</sub>Cl<sub>4</sub>N<sub>2</sub>NiO<sub>2</sub>(%): C, 46.47; H, 3.12; N, 5.42. Found (%): C, 47.13; H, 3.31; N, 5.14.

### 1.2.3 Synthesis of [Ni(3-Cl-salcy)] (2)

Complex **2** was prepared in a similar method as that of complex **1**, except the ligand 3-Cl-salcyH<sub>2</sub>

(0.024 5 g, 0.1 mmol) was used to replace 3,5-Cl-salcyH<sub>2</sub>. The red block crystals of **2** were afforded after one week. Yield: 42%. Anal. Calcd. For C<sub>20</sub>H<sub>18</sub>Cl<sub>2</sub>N<sub>2</sub>NiO<sub>2</sub> (%): C, 53.62; H, 4.05; N, 6.25; Found: C, 53.93; H, 4.12; N, 6.14.

### 1.3 X-ray crystal structure analysis

The data set of reflections were collected at 293(2) K on an Xcalibur Eos automated diffractometer with Mo *K*α radiation (λ=0.071 073 nm) and a low-temperature device Cryostream cooler (Oxford Cryosystem). Integration of the intensities and correction for Lorentz and polarization effects were performed using the CrysAlisPro software<sup>[21-22]</sup>. The central nickel atom was located by direct method, and successive Fourier syntheses revealed the remaining atoms. Refinements were achieved by the full-matrix method on *F*<sup>2</sup> using the Olex2 software package<sup>[23]</sup>. In the final refinement, all the non-H atoms were anisotropically refined. All H atoms were placed in calculated positions and refined using the riding model approximation. For the cyclohexane, C-H bonds were fixed at 0.097 nm, and the *U*<sub>iso</sub> values of the hydrogen atoms of methyl groups were set to 1.5*U*<sub>eqC</sub> and the *U*<sub>iso</sub> values of all other hydrogen atoms were set to 1.2*U*<sub>eqC</sub>, with aromatic C-H distances of 0.093 nm. The detailed crystal data and structure refinement for **1** and **2** are given in Table 1. Selective bond lengths and angles of **1** and **2** are listed in Table 2.

CCDC: 1892682, **1**; 1855958, **2**.

Table 1 Crystallographic data and structure refinement for complexes **1** and **2**

| Complex           | <b>1</b>  | <b>2</b>  |
|-------------------|---|---|
| Formula           | C <sub>20</sub> H <sub>16</sub> Cl <sub>4</sub> N <sub>2</sub> NiO <sub>2</sub> | C <sub>20</sub> H <sub>18</sub> Cl <sub>2</sub> N <sub>2</sub> NiO <sub>2</sub> |
| Formula weight    | 516.84  | 447.95  |
| Crystal system    | Monoclinic  | Triclinic   |
| Crystal size / mm | 0.20×0.18×0.16  | 0.18×0.14×0.12  |
| Space group       | <i>P</i> 2 <sub>1</sub> / <i>c</i>  | <i>P</i> $\bar{1}$  |
| <i>a</i> / nm     | 1.352 06(14)  | 1.174 51(8)   |
| <i>b</i> / nm     | 1.377 74(10)  | 1.287 43(8)   |
| <i>c</i> / nm     | 1.247 79(13)  | 1.356 64(8)   |
| α / (°)           |   | 86.447(5)   |
| β / (°)           | 117.130(13)   | 69.997(6)   |
| γ / (°)           |   | 76.885(6)   |

Continued Table 1

|   |                                  |                                  |
|---|----------------------------------|----------------------------------|
| Volume / nm <sup>3</sup>  | 2.068 6(3)                       | 1.877 1(2)                       |
| $D_c$ / (g·cm <sup>-3</sup> )                                       | 1.66                             | 1.585                            |
| $Z$   | 4                                | 1                                |
| $\mu$ / mm <sup>-1</sup>  | 1.475                            | 1.336                            |
| Reflection collected, unique ( $R_{int}$ )                          | 8 941, 3 518 (0.029 0)           | 13 206, 6 592 (0.066 6)          |
| Reflection with $I > 2\sigma(I)$                                    | 1 847                            | 2 695                            |
| $\theta$ range for data collection / (°)                            | 3.27~25.00                       | 3.34~25.00                       |
| Data, restraint, parameter  | 3 518, 0, 262                    | 6 592, 0, 487                    |
| Goodness-of-fit on $F^2$  | 1.047                            | 0.945                            |
| $R$ indices $[I > 2\sigma(I)]^{ab}$                                 | $R_1=0.034\ 7$ , $wR_2=0.072\ 1$ | $R_1=0.058\ 6$ , $wR_2=0.061\ 0$ |
| $R$ indices (all data)  | $R_1=0.050\ 4$ , $wR_2=0.080\ 8$ | $R_1=0.129\ 0$ , $wR_2=0.077\ 1$ |
| $(\Delta\rho)_{max}$ , $(\Delta\rho)_{min}$ / (e·nm <sup>-3</sup> ) | 393, -276                        | 409, -438                        |

$$^a R_1 = [|F_o| - |F_c|] / |F_o|; ^b wR_2 = [w(F_o^2 - F_c^2)] / [w(F_o^2)]^{1/2}.$$

Table 2 Selected bond lengths (nm) and angles for complexes **1** and **2**

| <b>1</b>                   |              |                          |              |                           |             |
|----------------------------|--------------|--------------------------|--------------|---------------------------|-------------|
| Ni(1)-O(2)                 | 0.184 57(18) | Ni(1)-O(1)               | 0.185 32(19) | Ni(1)-N(2)                | 0.185 1(2)  |
| Ni(1)-N(1)                 | 0.185 3(2)   | Ni(1)-Ni(1) <sup>i</sup> | 0.331 56(7)  | Cl(1)-C(4)                | 0.174 0(3)  |
| Cl(3)-C(2)                 | 0.173 4(3)   | Cl(2)-C(17)              | 0.174 5(3)   | Cl(4)-C(19)               | 0.173 3(3)  |
| O(2)-Ni(1)-N(2)            | 93.93(9)     | O(2)-Ni(1)-N(1)          | 179.74(10)   | O(2)-Ni(1)-O(1)           | 85.61(8)    |
| N(2)-Ni(1)-N(1)            | 85.81(10)    | N(2)-Ni(1)-O(1)          | 178.60(9)    | O(1)-Ni(1)-N(1)           | 94.64(9)    |
| C(3)-C(2)-Cl(3)            | 118.6(2)     | C(5)-C(4)-Cl(1)          | 119.8(3)     | C(1)-C(2)-Cl(3)           | 118.5(2)    |
| C(3)-C(4)-Cl(1)            | 119.5(3)     |                          |              |                           |             |
| <b>2</b>                   |              |                          |              |                           |             |
| Ni(1)-O(1)                 | 0.183 8(2)   | Ni(2)-O(3)               | 0.183 7(2)   | Ni(1)-O(2)                | 0.184 4(2)  |
| Ni(2)-O(4)                 | 0.184 4(2)   | Ni(1)-N(2)               | 0.184 7(3)   | Ni(2)-N(4)                | 0.184 6(3)  |
| Ni(1)-N(1)                 | 0.185 5(3)   | Ni(2)-N(3)               | 0.185 4(3)   | Ni(1)-Ni(1) <sup>ii</sup> | 0.352 97(2) |
| Ni(2)-Ni(2) <sup>iii</sup> | 0.338 07(10) | Cl(1)-C(2)               | 0.174 0(4)   | Cl(3)-C(22)               | 0.174 3(3)  |
| Cl(2)-C(19)                | 0.174 1(4)   | Cl(4)-C(39)              | 0.173 4(3)   |                           |             |
| O(1)-Ni(1)-O(2)            | 84.26(10)    | O(3)-Ni(2)-O(4)          | 84.02(10)    | O(1)-Ni(1)-N(2)           | 175.91(12)  |
| O(3)-Ni(2)-N(4)            | 178.18(12)   | O(2)-Ni(1)-N(2)          | 94.18(11)    | O(4)-Ni(2)-N(4)           | 94.24(11)   |
| O(1)-Ni(1)-N(1)            | 95.08(11)    | O(3)-Ni(2)-N(3)          | 94.90(11)    | O(2)-Ni(1)-N(1)           | 175.87(13)  |
| O(4)-Ni(2)-N(3)            | 178.35(12)   | N(2)-Ni(1)-N(1)          | 86.75(12)    | N(4)-Ni(2)-N(3)           | 86.86(12)   |

Symmetry codes: <sup>i</sup>  $-x+1, -y, -z$  for **1**; <sup>ii</sup>  $-x, 1-y, -z$ ; <sup>iii</sup>  $x, -y, 1-z$  for **2**.

## 2 Results and discussion

### 2.1 Structure description

The identity of **1** and **2** were elucidated by single-crystal X-ray diffraction, elemental analysis results of were fully consistent with the crystallographic formulation. Single-crystal X-ray diffraction reveals that complex **1** crystallizes in the monoclinic  $P2_1/c$

(No.14) space group, which unit cell contains one crystallography independent Ni(II) forming two racemic neutral monomers [Ni((+)-3,5-Cl-salcy)] and [Ni((-)-3,5-Cl-salcy)]. As shown in Fig.1, the central Ni(II) exhibits tetra-coordinated environment which is defined by  $[N_2O_2]$  in the equatorial plane from Schiff-base ligand. The bond lengths of Ni-O(N) are in a range of 0.183 7(3)~0.185 5(4) nm, and bond angles of O(N)-

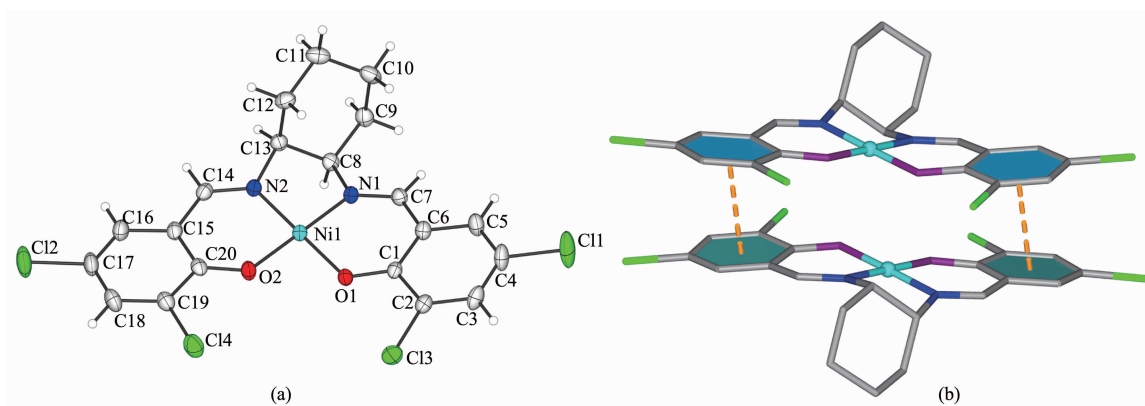
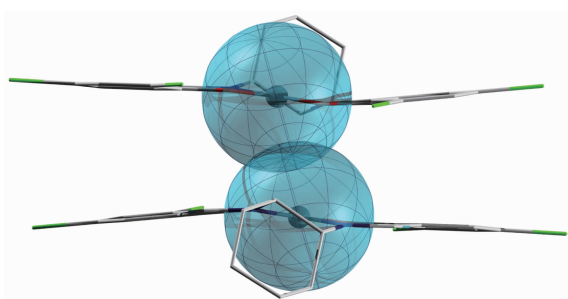


Fig.1 (a) Asymmetric unit of **1** with displacement ellipsoids drawn at 30% probability level; (b)  $\pi \cdots \pi$  non-bonding contact of self-assembled supramolecular dimer built up by symmetry operation:  $1-x, -y, -z$

Ni-O vary from  $84.23(15)^\circ$  to  $178.38(16)^\circ$ , which are favorably comparable with the corresponding values observed in salen-type Ni(II) analogous<sup>[24-25]</sup>.

The dihedral angle calculated between the planes of two benzene rings for **1** is  $8.23(10)^\circ$ , thus, the whole molecule exhibit coplanar configuration. Owing to the  $\pi$ - $\pi$  interactions (the distances of  $\text{Cg1}^i \cdots \text{Cg1}$  and  $\text{Cg2}^i \cdots \text{Cg2}$  are equal to each other with centroid-to-centroid distance of  $0.387\ 4(32)$  nm,  $\text{Cg1}$ : centroid of C1~C6 ring,  $\text{Cg3}$ : C15~C20 ring, Symmetry code:  $^i\ 1-x, -y, -z$ ), two neighboring molecules are further linked to each other to form a self-assembled supramolecular dimer (Fig.1(b)), in which the Ni $\cdots$ Ni distance of *ca.*  $0.331(26)$  nm (Fig.2) is smaller than the sum of two nickel atoms' van der Waals radius<sup>[26]</sup>.



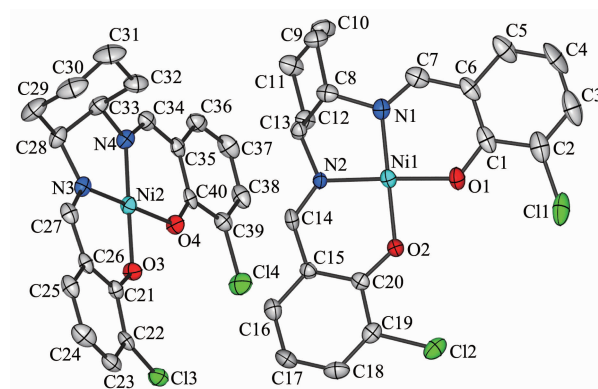
van der Waals radius for Ni atom: 200 pm

Fig.2 Ni $\cdots$ Ni no bond interactions in **1**, built up by symmetry operation:  $1-x, -y, -z$

It is noteworthy that according to the analysis result of PLATON software<sup>[27]</sup>, except  $\pi$ - $\pi$  interactions, there is not any classical or unclassical hydrogen bond in the crystal structure. By comparison, Hirshfeld surface gives us qualitative and quantitative

contributions of the interactions in the crystal packing. Detailed discussion is addressed in Hirshfeld surface analysis section.

Complex **2** crystallizes in the triclinic  $P\bar{1}$  (No.2) space group, and its asymmetric unit contains two identical, but crystallographically independent mononuclear Ni(II) unit. The Ni(II) centers present same coordination environment with **1** by chelating with chloride salen-type ligand via  $[\text{N}_2\text{O}_2]$  in the equatorial plane. The bond lengths of Ni-O and Ni-N in the two Ni(II) moieties are in a range of  $0.183\ 7(2)\sim 0.184\ 4(2)$  nm and  $0.184\ 6(3)\sim 0.185\ 5(3)$  nm, respectively. The bond angles around Ni(II) centers have been found to be  $84.02(10)^\circ$  to  $94.90(11)^\circ$ , respectively (Fig.3).



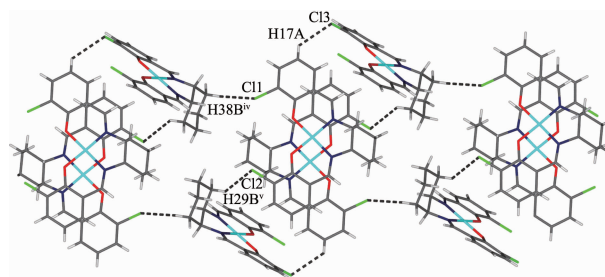
Displacement ellipsoids are drawn at the 40% probability level; H atoms are omitted for clarity

Fig.3 Molecular structure of **2** showing the atom-labeling scheme

Intermolecular interaction analysis shows that the distance between  $\text{Cg1}^{\text{ii}} \cdots \text{Cg1}$  is equal to  $\text{Cg2}^{\text{ii}} \cdots \text{Cg2}$  (Symmetry code:  $^{\text{ii}}\ -x, 1-y, -z$ ) and  $\text{Cg3}^{\text{iii}} \cdots \text{Cg3}$  is

equal to  $\text{Cg4}^{\text{iii}} \cdots \text{Cg4}$  (Symmetry code:  $^{\text{iii}} x, -y, 1-z$ ), with centroid-to-centroid distance being 0.419 6(2) and 0.382 2(2) nm, respectively, where Cg1, Cg2, Cg3 and Cg4 are the centroids of the C1~C6, C5~C20, C21~C26 and C35~C40, respectively. Beside these offset  $\pi$ - $\pi$  stacking created by neighboring monomers, hydrogen bonds formed by phenolic oxygen atoms also play an important part in linking the neighboring racemic monomers to form self-assembled supramolecular dimers ( $\text{C8-H8} \cdots \text{O1}^{\text{iii}}$ :  $\text{D} \cdots \text{A}$  0.339 3(5) nm,  $\text{D-H} \cdots \text{A}$  145°). According to the analysis result of PLATON software<sup>[27]</sup>, although there is no classic H-bond interactions in **2**, C-H $\cdots$ Cl hydrogen bonds play a key role in stabilizing the crystal structure. As illustrated in Fig.4, the adjacent monomers are

connected by multiple C-H $\cdots$ Cl hydrogen bonds interactions to generate a two-dimensional layered structure. Detailed hydrogen-bond geometry information is summarized in Table 3.



Symmetry codes:  $^{\text{iv}} -1+x, 1+y, z$ ;  $^{\text{v}} -x, 1-y, -z$ ; Intramolecular hydrogen bonds are shown as a dashed line

Fig.4 Two-dimensional layer structure of complex **2** formed by intramolecular hydrogen bonding

Table 3 PLATON analysis result of hydrogen bond parameters for complex **2**

| D-H $\cdots$ A              | $d(\text{D-H})$ / nm | $d(\text{H}\cdots\text{A})$ / nm | $d(\text{D}\cdots\text{A})$ / nm | $\angle \text{DHA}$ / (°) |
|-----------------------------|----------------------|----------------------------------|----------------------------------|---------------------------|
| C(8)-H(8) $\cdots$ O(1)     | 0.098                | 0.254                            | 0.339 3(5)                       | 145                       |
| C(17)-H(17) $\cdots$ Cl(3)  | 0.093                | 0.276                            | 0.342 9(4)                       | 130                       |
| C(29)-H(29B) $\cdots$ Cl(2) | 0.097                | 0.278                            | 0.372 4(4)                       | 163                       |
| C(32)-H(32B) $\cdots$ Cl(1) | 0.097                | 0.283                            | 0.358 7(4)                       | 136                       |

## 2.2 IR absorbance spectrum

The IR spectra of the complexes are very similar in the given region, and therefore, the spectrum of complex **1** is described here representatively. The IR spectrum (Fig.5) showed a broad band centered in a range of 2 950~2 850  $\text{cm}^{-1}$  and a strong peak at 1 447  $\text{cm}^{-1}$  are assigned to  $\nu(\text{-CH}_2\text{-})$  vibrations indicating the presence of  $\text{-CH}_2\text{-}$  group of the cyclohexane unit. The strong peak at 1 632  $\text{cm}^{-1}$  corresponds to the vibration of the C=N bonds. The characteristic peaks at 1 132

and 575  $\text{cm}^{-1}$  are attributed to the vibrations of  $\nu(\text{Ni-O})$  and  $\nu(\text{Ni-O})$ , respectively, and the peak at 729  $\text{cm}^{-1}$  is attributed to the  $\nu(\text{C-Cl})$ . These results are consistent with the structural analysis.

## 2.3 Hirshfeld surface analysis

The bundle of inter-related weak molecular interactions is difficult to be unraveled by traditional methods<sup>[28]</sup>. Hirshfeld surface analysis provides us a new perspective on the issue. This analysis method can provide detailed explanation about the nearby environment of the molecules in a crystal, and the comparison between similar structures can give a more specific description of the difference<sup>[29]</sup>. Although hydrogen bond interaction formed by halogen is weak and cannot be easily find out by traditional methods, Hirshfeld surface in the 2D fingerprint plots show that, for complex **1**, the  $\text{Cl}\cdots\text{H-C}$  interaction (Fig.6a) covers the highest proportion (42.5%) of the total plots, whereas the  $\text{C}\cdots\text{H-C}$  (Fig.6b) contacts only cover less than a third proportion of  $\text{Cl}\cdots\text{H-C}$  interaction (14.0%). These results indicate that the

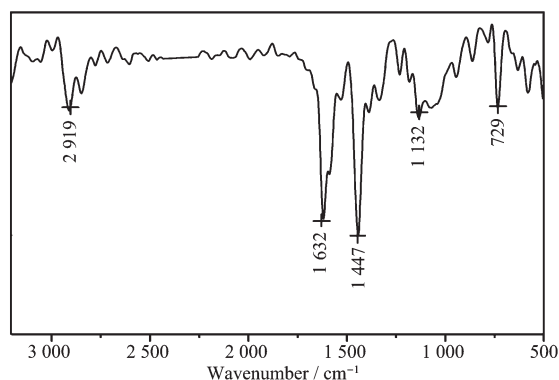
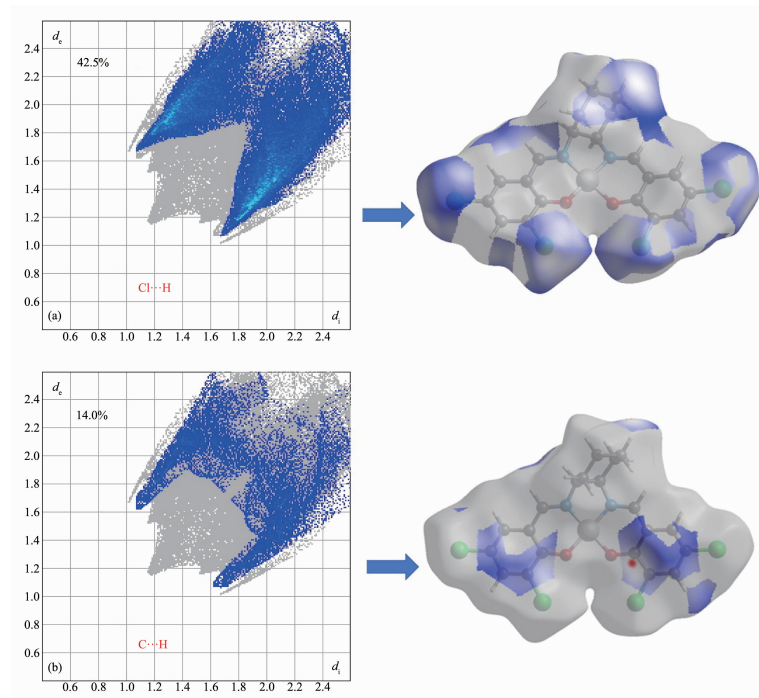


Fig.5 IR spectrum of **1**



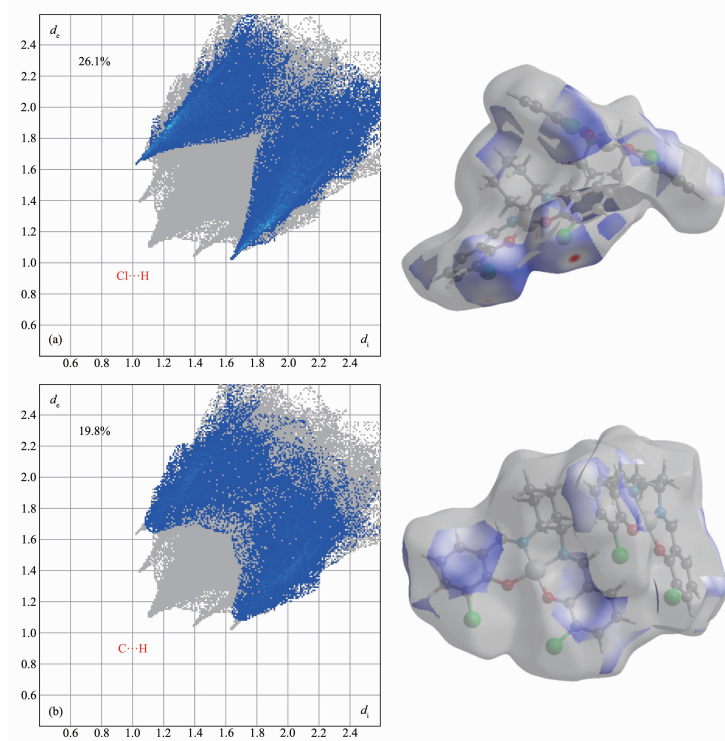
halogen atoms in **1** play the most important part in stabilizing the solid stature.

As shown in Fig.7,  $\text{Cl}\cdots\text{H}/\text{H}\cdots\text{Cl}$  bonding still appears to be a major contributor in the crystal



Surfaces in the right hand columns highlight the relevant surface patches associated with the specific contacts in the total Hirshfeld surface area of the complex

Fig.6 Two-dimensional fingerprint plots of complex **1** resolved into  $\text{Cl}\cdots\text{H}/\text{H}\cdots\text{Cl}$  (a) and  $\text{C}\cdots\text{H}/\text{H}\cdots\text{C}$  (b)



Surfaces in the right hand columns highlight the relevant surface patches associated with the specific contacts in the total Hirshfeld surface area of the complex

Fig.7 Two dimensional fingerprint plots of complex **2** resolved into  $\text{Cl}\cdots\text{H}/\text{H}\cdots\text{Cl}$  (a) and  $\text{C}\cdots\text{H}/\text{H}\cdots\text{C}$  (b) contacts

packing of **2**, and the proportion is significantly lower than that in **1**, merely comprising 26.1% of the total Hirshfeld surfaces, whereas C $\cdots$ H/H $\cdots$ C close contacts contribution appear higher in the 2D fingerprint plot (19.8%). These results indicate that although the structure and composition of **2** is similar with **1**, different substitution number of chlorine atoms may result in an entirely different intermolecular interactions in solid structures.

### 3 Conclusions

In summary, two new salen-type halogenated Schiff-base Ni(II) complexes have been synthesized by conventional method. The structures of the complexes were determined by single-crystal X-ray diffractions. A detailed comparison of Hirshfeld surface analysis result indicate that although the interaction formed by halogen atom is weak, halogen atoms can play an important role in supramolecular interaction. As different supramolecular interaction can lead a totally different physicochemical properties, further work will continue focus on the synthesis of halogenate ligands constructed complexes to systematically explore the regulating effect of halogen atoms.

**Acknowledgement:** This work was supported by Fund for Less Developed Regions of the National Natural Science Foundation of China (Grant No.31760257); Joint Research Projects of Yunnan province of Local of institutions (partial) of higher education (Grant No.2017FH001-002); Agricultural plastic film and products research and development of Plateau area (Grant No.2016DH006); The Kunming University Chemistry & Chemical engineering students' science and technology innovation project (Grant No.HXHG1808).

### References:

- [1] Huang F H, Anslyn E V. *Chem. Rev.*, **2015**, *115*:6999-7000
- [2] Slater A G, Perdigo L M A, Beton P H, et al. *Acc. Chem. Res.*, **2014**, *47*:3417-3427
- [3] Stupp S I, Palmer L C. *Chem. Mater.*, **2014**, *26*:507-518
- [4] LI Zhi-Jun(李志军), ZHANG Jing(张静), WEI Xue-Hong(魏学红), et al. *Chinese J. Inorg. Chem.*(无机化学学报), **2018**, *34*:353-358
- [5] Aakery C B, Beatty A M, Helfrich B A. *Angew. Chem. Int. Ed.*, **2010**, *40*:3240-3242
- [6] Guillermin V, Kim D, Eubank J F, et al. *Chem. Soc. Rev.*, **2014**, *43*:6141-6172
- [7] Perry J J, Perman J A, Zaworotko M J. *Chem. Soc. Rev.*, **2009**, *38*:1400-1417
- [8] Iyer R S, Rowland F S. *Chem. Phys. Lett.*, **1973**, *21*:346-348
- [9] Wernsdorfer W, Aliagaalcalde N, Hendrickson D N, et al. *Nature*, **2002**, *416*:406-409
- [10] Lecren L, Wernsdorfer W, Li Y G, et al. *J. Am. Chem. Soc.*, **2007**, *129*:5045-5051
- [11] Saha B K, Jetti R K R, Reddy L S, et al. *Cryst. Growth Des.*, **2005**, *5*:887-899
- [12] Bertani R, Sgarbossa P, Venzo A, et al. *Coord. Chem. Rev.*, **2010**, *254*:677-695
- [13] Ma C, Tian G, Zhang R. *J. Organomet. Chem.*, **2006**, *691*:2014-2022
- [14] Mad'Arová M, Sivák M, Kuchta L, et al. *Dalton Trans.*, **2004**:3313-3320
- [15] Xie Y S, Jia N, Zheng F K, et al. *Cryst. Growth Des.*, **2009**, *9*:118-126
- [16] Hazari A, Gómez-García C J, Drew M G B, et al. *Polyhedron*, **2017**, *138*:145-153
- [17] Wu Q, Pu Q, Wu Y M, et al. *J. Coord. Chem.*, **2015**, *68*:1010-1020
- [18] Miyasaka H, Saitoh A, Abe S. *Coord. Chem. Rev.*, **2007**, *251*:2622-2664
- [19] DONG Wen-Kui(董文魁), LÜ Zhong-Wu(吕忠武), Sun Yin-Xia(孙银霞), et al. *Chinese J. Inorg. Chem.*(无机化学学报), **2009**, *25*:1627-1634
- [20] YOU Wei(游伟), YAO Cheng(姚成), HUANG Wei(黄伟). *Chinese J. Inorg. Chem.*(无机化学学报), **2010**, *26*:867-874
- [21] *CrysAlisPro Software System, Ver.1.171.38.41*, Agilent Technologies UK Ltd, Oxford, UK, **2015**.
- [22] *CrysAlisPro*, Abingdon, Oxfordshire, England, **2006**.
- [23] Dolomanov O V, Bourhis L J, Gildea R J, et al. *J. Appl. Crystallogr.*, **2010**, *42*:339-341
- [24] Houjou H, Hoga Y, Ma Y L, et al. *Inorg. Chim. Acta*, **2017**, *461*:27-34
- [25] Guo T L, Gou Y, Guo M X, et al. *Synth. React. Inorg. Met.-Org. Chem.*, **2015**, *45*:327-332
- [26] Batsanov S S. *Inorg. Mater.*, **2001**, *37*:871-885
- [27] Spek A L. *J. Appl. Crystallogr.*, **2003**, *36*:7-13
- [28] Spackman M A, Jayatilaka D. *CrystEngComm*, **2009**, *11*:19-32
- [29] McKinnon J J, Jayatilaka D, Spackman M A. *Chem. Commun.*, **2007**:3814-3816